INTERNATIONAL JOURNAL FOR NUMERICAL METHODS IN ENGINEERING, VOL. 28, 1703–1713 (1989)

# 3-D BOUNDARY ELEMENT METHOD FOR CRACKS IN A PLATE

N. FARES*

*Rensselaer Polytechnic Institute, Troy, New York 12180—3590, U.S.A.*

V. C. LI†

*Massachusetts Institute of Technology, Cambridge, Massachusetts 02139, U.S.A.*

## SUMMARY

New fundamental solutions which automatically satisfy boundary conditions at the interfaces of an elastic plate perfectly bonded to two elastic halfspaces are implemented in a 3-D boundary element method (BEM) for crack problems. The BEM features a new integration scheme for highly singular kernels. The capability is achieved through a part analytic and part numerical integration procedure, such that the analytic part of the integration is similar for all slip/opening variations. 'Part-through' elliptic cracks in an elastic plate with traction-free surfaces are analysed and the stress intensity factor (SIF) values along the crack front are found to compare favourably with widely accepted numerically obtained SIF results by Raju and Newman.[1]

## INTRODUCTION

Numerical methods based on integral equations are often used in 3-D linear elastic fracture mechanics as an alternative to the more popular finite element method.[2–8] Different integral equation formulations use a variety of kernels or fundamental solutions such as point force and nuclei of strain elastic fields. In addition, numerical implementations of the same formulation may make different assumptions concerning the unknown displacements or displacement discontinuities and tractions over the crack surface. In some cases the unknown field variables along the boundary may be assumed to be continuous and differentiable, while in other cases they may be assumed to be piecewise continuous and differentiable with lines along which discontinuities may occur. Examples of integral equation based numerical methods are the boundary element method, boundary integral equations method and body force method.

In some integral equation formulations, special kernels (or fundamental solutions) are used which automatically satisfy boundary conditions on external boundaries. In such formulations, discretization is required only on the crack surfaces. Elliptic and semi-elliptic cracks in a halfspace with a traction-free surface or in a region consisting of two bonded halfspaces have been extensively studied using such specialized fundamental solutions.[9–11]

A common difficulty of integral equation formulations dealing with crack problems is the accurate evaluation of singular integrals. The singular integrals encountered in 3-D crack

*Research Assistant Professor of Civil Engineering. Formerly Research Fellow in the Division of Applied Sciences at Harvard University

†Associate Professor of Civil Engineering

0029–5981/89/071703–11$05.50


*Received 20 August 1988*
*Revised 6 December 1988*

formulations vary with the fundamental solutions used. In classical boundary element formulations, the singular integrals involved are of the principal value kind. Principal value integration techniques have been dealt with by a variety of methods including semi-analytic evaluations,[12] mapping techniques[8] and quadrature formulae.[13,14] In the body force method, the evaluation of singular integrals which are more singular than principal value integrals is needed. The highly singular integrals are known as finite part integrals.[15-17] Murakami and Nemat-Nasser[9] described a part analytic and part numerical method to evaluate these highly singular integrals, while Kutt[18] developed Gaussian-type quadrature formulas for one dimensional (useful in 2-D problems) finite part integration.

This paper will present a numerical implementation of an integral equation formulation to solve cracks in a plane layered region (Figure 1). The integral equation formulation and discretization will first be presented. The presentation will emphasize a new finite part integration scheme. Next, some numerical studies on circular and elliptic cracks in infinite space will highlight the discretization requirements for accurate results. The studies will focus on the region adjacent to the crack front. Finally, computed stress intensity factors for 'part-through' semi-elliptic cracks in an elastic plate (upper and lower surfaces traction free) will be used as an example of the capability of the method. The resulting 'part-through' crack results are found to compare favourably with the widely accepted finite element solutions by Raju and Newman[1] of the same problem.

## DESCRIPTION OF THE METHOD

The present numerical method can be formally classified as either an indirect boundary element method[19] or a 3-D displacement discontinuity method.[20] The required fundamental solutions correspond to nuclei of strain elastic fields in a layered medium with two interfaces. The nuclei of strain elastic fields in such media were recently derived by Fares.[21] The advantage of using the specialized nuclei of strain solutions is that the boundary conditions on the interfaces (shown in Figure 1) are automatically satisfied. Hence, only the crack surface needs to be discretized. The method relies on the following integral representation of the stress $\sigma_{pq}$ due to an applied stress

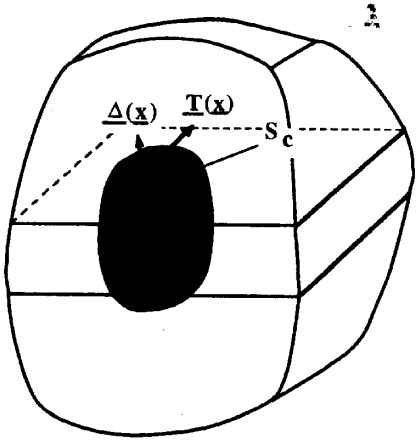


Figure 1. A layered elastic region with two interfaces containing a crack. Tractions and displacement jumps $\Delta_j$ are defined over the surface $S_c$

$\sigma_{pq}^{\text{applied}}$ and a distribution of opening and sliding ($\Delta_i$) on a crack surface $S_c$:

$$\sigma_{pq}(\mathbf{x}) = \sigma_{pq}^{\text{applied}}(\mathbf{x}) - \int_{S_c} G_{ji}^{pq}(\mathbf{x}, \mathbf{x}') \cdot n_j^+(\mathbf{x}') \cdot \Delta_i(\mathbf{x}') \cdot \mathrm{d}S \tag{1}$$

where the fundamental solution $G_{ji}^{pq}(\mathbf{x}, \mathbf{x}')$ is the stress at a point $\mathbf{x}$ due to a nucleus of strain in a layered medium at point $\mathbf{x}'$, and $\mathbf{n}^+(\mathbf{x})$ is the vector normal to the upper crack surface. The integral in (1) is carried out over the crack surface $S_c$.

The integral in (1) is well defined for any field point $\mathbf{x}$ in space not lying on the crack surface. When a point $\mathbf{x}$ lies on $S_c$ the integral in (1) must be interpreted as an integral with the limit of a point $\mathbf{x}^*$ not lying on $S_c$ approaching $\mathbf{x}$. Moving the limit operator inside the integral leads to a 'finite part' integral in the Hadamard sense. The discretization and numerical solution of the singular integral equations obtained from (1) when boundary conditions (involving $\sigma_{pq}$ and $\Delta_j$ on $S_c$) are given will be described next.

The opening and sliding $\Delta_j(\mathbf{x})$ along a crack surface (assumed planar) are parametrized with respect to local co-ordinates in subregions of the crack surface. The subregions are defined by one or several straight edged triangles. Therefore the discretization assumption allow discontinuities in $\Delta_j(\mathbf{x})$ to occur along some line segments on $S_c$.

The piecewise definition of unknown field variables is common in boundary (and finite) element methods. However, the present implementation has two characteristics. First, the unknown parameters discretizing $\Delta_j(\mathbf{x})$ are not associated with nodal values. Second, the shape functions that locally define $\Delta_j(\mathbf{x})$ are defined with respect to real space (possibly rotated and translated) co-ordinates instead of parametrized co-ordinates. These characteristics allow the implementation of crack front subregions (or elements) in the following way. Assume a crack lies in the plane $z=0$. The orientation of the local $y$-co-ordinate system at triangles containing a segment of the crack front is chosen to be perpendicular to the crack front. $\Delta_j(\mathbf{x})$ at the border regions is then parameterized as a polynomial expression of (local) $x$ and $y$ multiplied by $\sqrt{y}$ to obtain theoretically acceptable crack front opening or sliding variations.

Once the variation of $\Delta_j(\mathbf{x})$ is specified, boundary conditions are satisfied at a discrete number of points (called collocation points). The number of collocation points should equal the total number of parameters characterizing $\Delta_j(\mathbf{x})$. If the boundary conditions are linear, an algebraic system of equations is obtained whose solution yields the parameters used to discretize $\Delta_j(\mathbf{x})$. Once $\Delta_j(\mathbf{x})$ is known on $S_c$, displacements and stresses can be obtained at any point in space and stress intensity factors can be obtained at any point on the crack front. The stress intensity factors $K_I$, $K_{II}$ and $K_{III}$ are obtained using the classical asymptotic relations between crack opening near a crack tip and the value of stress intensity factors for plane strain (in the case of $K_I$ and $K_{II}$) and antiplane (in the case of $K_{III}$) deformations. In setting up the system of equations discussed above, a discretized version of the integrals in (1) has to be evaluated, and will be discussed next.

The kernels $G_{ji}^{pq}(\mathbf{x}, \mathbf{x}')$ in (1) can be derived (or computer generated) using the method outlined by Fares and Li.[22] The full expressions are given in Fares.[21] The singular part of the kernels used in the case of tensile cracks is the same as the infinite space tensile cracks kernels used in the body force method by Murakami and Nemat-Nasser.[9] An example of the method of integrating the infinite space crack kernels will be discussed in this paper. Formulas of the integration scheme for the required singular integrals (both for the tensile and shear cracks) are given in the Appendix. Further details are discussed in Fares.[21]

The integrals in the case of the infinite space tensile cracks are of the form

$$\lim_{z \to 0} \int\int_{S_c} f(x, y) \cdot \left[ \frac{1}{r^3} - 3 \cdot z^2 \cdot \frac{1}{r^5} \right] \cdot \mathrm{d}x\mathrm{d}y \tag{2}$$

where $f(x, y)$ is a smooth function, $S_c$ is a planar surface with $z=0$ and $r^2=x^2+y^2+z^2$. The above form can be applied to an arbitrary planar surface by defining conveniently translated and rotated local $x$, $y$, $z$ co-ordinates.

If the origin does not lie on $S_c$ then the integral (2) is not singular and an integration scheme similar to that described by Murakami and Nemat-Nasser[9] is used. If the origin lies on $S_c$ then integral (2) is a finite part integral and is treated in the following manner. First $f(x, y)$ is represented as the sum of the Taylor expansion of $f(x, y)$ around the origin up to parabolic terms plus a residue (say $f^*(x, y)$). The residue $f^*(x, y)$ multiplied by the kernel is non-singular and can be treated using regular quadrature methods. The constant, linear and parabolic terms of the Taylor expansion of $f(x, y)$ multiplied by the kernel in (2) are each transformed into the sum of two non-singular line integrals which are evaluated numerically and a one dimensional finite part integral which is evaluated analytically. For example, the constant term (taken to be unity) is transformed by the following steps:

$$\lim_{z\to 0}\iint_{S_c}\left[\frac{1}{r^3}-3\cdot z^2\cdot\frac{1}{r^5}\right]\cdot dx\,dy=\int_{C^+}\frac{x-R}{y^2R}dy+\int_{C^-}\frac{x+R}{y^2R}dy$$
$$+2\cdot\lim_{z\to 0}\int_{y_{min}}^{y_{max}}\left[\frac{2\cdot z^2}{(y^2+z^2)^2}-\frac{1}{y^2+z^2}\right]\cdot dy \qquad (3)$$

where $R^2=x^2+y^2$ and $y_{min}$ and $y_{max}$ are depicted in Figure 2. Note that $(x+R)/y^2R$ are the limits as $z->0$ of indefinite integrals with respect to $x$ of $1/r^3$ such that the line integrands in (3) are non-singular. However, both line integrals in (3) have removable singularities (the integrands tend to a finite limit) when they cross the $y=0$ axis. The last integral in (3) contains the terms that were subtracted or added to the first two line integrals to make them non-singular. This last integral can be evaluated analytically as a non-singular integral if the limit operation is performed after integration or as a finite part integral if the limit operation is performed before integration. In any case the evaluation of the last integral gives

$$-2\cdot\left[\frac{1}{y_{max}}-\frac{1}{y_{min}}\right] \qquad (4)$$

Other finite part integration formulas required with this integration scheme are given in the Appendix. It is to be emphasized that no truncation of the Taylor expansion of $f(x, y)$ is assumed

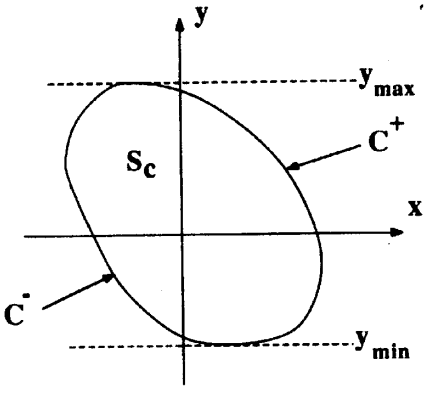


Figure 2. An integration region used to illustrate the finite part integration scheme

since $f^*(x, y)$ is also to be evaluated. The decomposition outlined above is simply a means of isolating the singular integrals in order to effectively treat them.

## NUMERICAL STUDIES

In this section, the discretization requirements for accurate stress intensity factor (SIF) results will be investigated, after which a few example problems will be solved. For the discretization requirement studies, the crack considered is circular and lies in infinite space under mode I loading. The analytic solution of this problem is known.[23] Two aspects of discretization near the crack front region will be investigated. These aspects are the choice of the orientation of lines along which $\Delta_j(x)$ may be discontinuous and the effect of approximating a non-straight crack line with straight line segments.

Consider a penny-shaped crack discretized into identical angular sectors. Two different subdivisions of a representative sector into triangles are shown in Figures 3(a) and (b). In Figure 3(a), triangles 1–6 have $\sqrt{y_L}$ and $y_L \cdot \sqrt{y_L}$ opening variations (with two parameters specifying the magnitudes) such that triangles 1–2, 3–4 and 5–6 have local axes 1, 2 and 3 respectively. Triangles 7, 8 and 9 and triangle 10 have a parabolic variation in $y_L$ (local axis 4) which implies a total of eight parameters used in the discretization corresponding to Figure 3(a). Figure 3(b) is similarly discretized with 8 parameters. $\sqrt{y_L}$ and $y_L \cdot \sqrt{y_L}$ opening variations are specified over triangles 1–5 such that triangles 1–2, 3 and 4–5 have local axis 1, 2 and 3 respectively. Triangles 6, 7 and 8 and triangle 9 have a parabolic variation in $y_L$ (local axis 4) in Figure 3(b). The number of line segments used to discretize the crack boundary is the same (24 segments) in both Figures 3(a) and (b). The only difference between the discretization of Figures 3(a) and (b) is that the lines along which $\Delta_j(x)$ can be discontinuous lie perpendicular to the crack boundary in Figure 3(a), whereas they lie at an angle to the boundary in Figure 3(b). The errors in the SIF obtained are 6·1 per cent and 9·8 per cent for Figures 3(a) and (b) respectively. By increasing the number of line segments used to discretize the crack front (with the same number of parameters), the error in a discretization similar to Figure 3(a) can be reduced to less than 1·5 per cent, while that error remains above 5 per cent in a discretization scheme similar to Figure 3(b). Therefore, in order to obtain accurate results using the present scheme, near the crack front it is necessary to orient lines along which $\Delta_j(x)$ can be discontinuous to lie perpendicular to the crack boundary. The importance of this condition is that in satisfying it, the assumed $\Delta_j(x)$ field is continuous when no variation of the SIF occurs along the crack front.

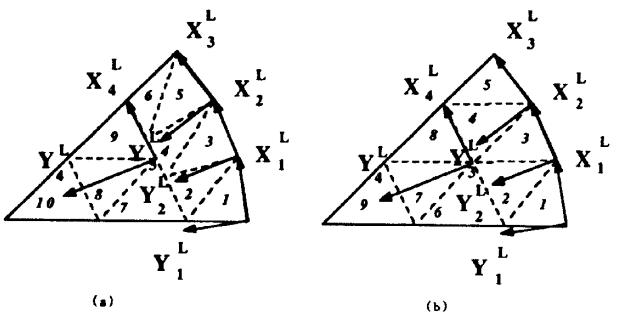


Figures 3(a) and (b). Two different types of discretization of a representative sector of a penny-shaped crack. See text for details

The errors in SIF as the number of line segments discretizing the crack front increases (using the subdivision method of Figure 3(a) with a total of only eight parameters) is as follows. Corresponding to 24, 36 48, 72 and 96 line segments the errors in SIF's are 6·1, 4·8, 2·5, 1·8 and 1·2 per cent respectively. Using Gao and Rice's[24] results to estimate the average first order variation in SIF due to the straight line segments' discretization of the crack boundary we obtain

$$\% \text{ error} \approx \frac{100\pi^2}{8n} \tag{5}$$

Using (5), the per cent errors in SIF for 24, 36, 48, 72 and 96 line segments are 5·1, 3·4, 2·6, 1·7 and 1·3 per cent respectively. The numerical results are consistent with the theoretical estimates. This study shows that the convergence rate of the average SIF at a straight line segments' discretization of a curved boundary to the SIF at the curved boundary is very slow. However, preliminary studies show that, if the discretization allows the SIF to vary along the straight line segments, the SIF at the midpoint of the segments converges faster to the SIF at the corresponding points on the curved boundary than do the corresponding average values. Hence, in the examples to be presented next, the parameters used to represent $\Delta_j(x)$ allow the SIF's to vary at least piecewise linearly along the crack front, and only midpoint SIF values are reported.

The first example problem is an elliptic crack in infinite space with an aspect ratio of 2 to 1 under tension. The discretization of a quarter of the crack is shown in Figure 4 (with symmetry assumed). The lines along which $\Delta_j(x)$ can be discontinuous have been carefully chosen to lie perpendicular to the boundary (i.e. the common segments between triangles 2–3, 4–5, 6–7, etc.). Fifty four parameters (degrees of freedom) were used to obtain the results of Figure 5. The analytic results are from Tada *et al.*[23] Note that good accuracy has been obtained in spite of the coarse discretization used in the inner region of the crack.

Finally, using this BEM, SIF's of 'part-through' semi-elliptic cracks in a plate will be presented. These examples show the BEM implementation of nuclei of strain elastic fields in a layered region with two interfaces. The rigidity of the upper and lower halfspaces is set to zero to obtain traction-free surfaces. For conciseness, one penetration depth and three aspect ratios of semi-elliptic cracks will be considered. Referring to the insets in Figures 6, 7 and 8, the penetration depth $a/H = 0{\cdot}2$ and the aspect ratios $a/c = 0{\cdot}4$, 1·0 and 2·0 respectively. Figure 9 is an example of the geometric discretization used and corresponds to aspect ratio $a/c = 2{\cdot}0$. The number of line segments discretizing the crack fronts are 9, 13 and 13 line segments per quadrant corresponding to the results shown in Figures 6, 7 and 8 respectively with a total of 46, 67 and 67 parameters (degrees of freedom) respectively. No effort has been made to resolve the singularities near the intersection of

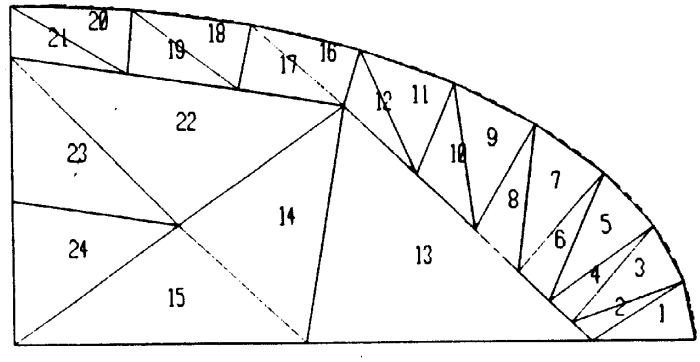


Figure 4. The discretization of a representative quadrant of an ellipse with aspect ratio of 2:1

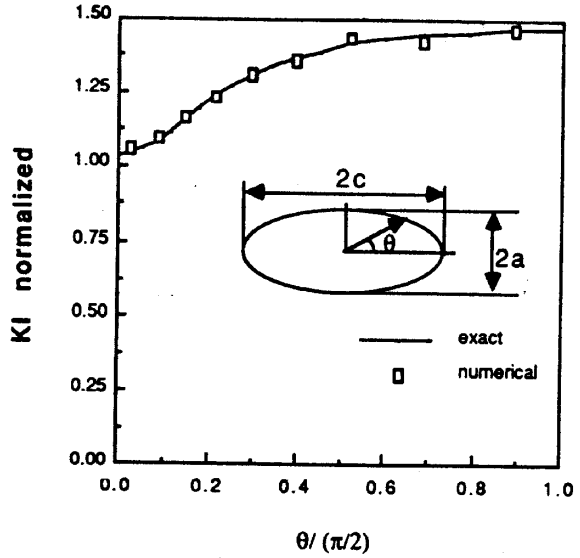


Figure 5. Comparison of numerically obtained stress intensity factors (SIF) of elliptic crack in infinite space problem with exact analytic solutions (e.g. Tada *et al.*[23]). $a/c = 0{\cdot}5$ and $\theta$ is as shown in inset. The SIF values are normalized by $\sigma\sqrt{a}$

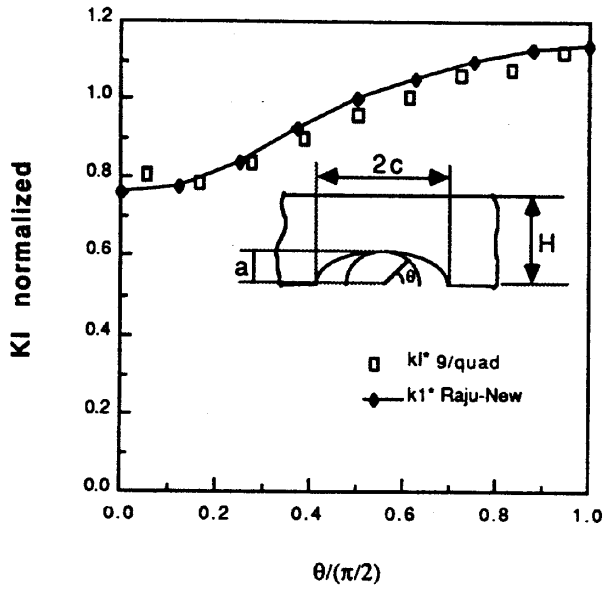


Figure 6

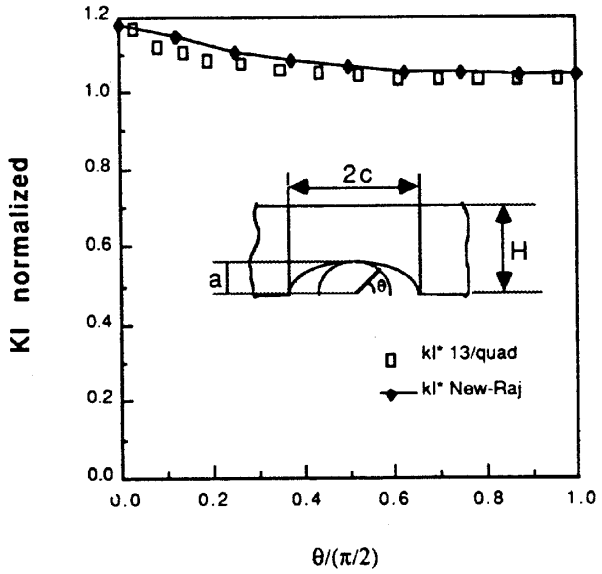


Figure 7

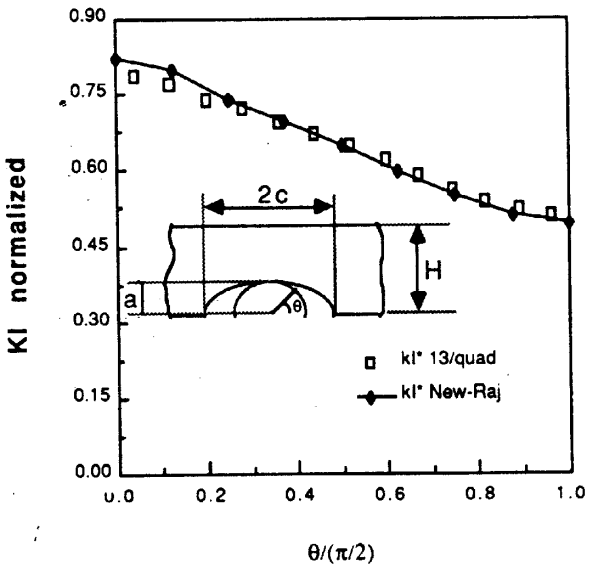


Figures 6, 7 and 8. Comparisons of numerically obtained stress intensity factors (SIF) of 'part-through' cracks in a plate using the present boundary element method scheme with widely accepted finite element results by Raju and Newman.[1] The agreement is good in all three cases with $a/H = 0{\cdot}2$ and $a/c = 0{\cdot}4$, $1{\cdot}0$ and $2{\cdot}0$ corresponding to Figures 6, 7 and 8 respectively ($\theta$ is as shown in inset). Following Raju and Newman,[1] the SIF values are normalized by $\sigma\sqrt{\pi a}/E(k)$ where $E(k)$ is the complete elliptic integral of the second kind, and $k^2 = 1 - c^2/a^2$ if $a/c \leqslant 1$ and $1 - a^2/c^2$ if $a/c > 1$

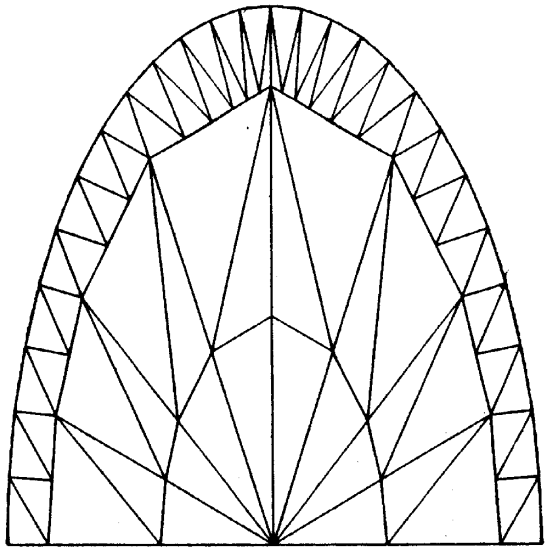

Figure 9. The discretization of a semi-elliptic crack with aspect ratios of 2:1

the crack surface with the traction-free interface. The results show reasonable agreement with the widely accepted finite element solutions by Raju and Newman.[1]

## CONCLUSION

An indirect BEM implementing recently derived nuclei of strain elastic fields was used to solve crack problems in infinite space and in a plane layered media. The formulation presented a new finite part integration scheme. Numerical studies on circular cracks were used to determine the discretization requirements. 'Part-through' elliptic crack problems in an elastic plate were solved to show the capability of the method. Comparison with available 3-D finite element solutions provide confidence in the accuracy of the present BEM.

### ACKNOWLEDGEMENTS

The authors acknowledge support of this work from the Crustal Dynamics Program at the National Aeronautics and Space Administration to the Massachusetts Institute of Technology.

## APPENDIX

In this Appendix, finite part integration formulas needed in the implementation of the BEM are given. All integrands on the right hand side are to be interpreted as finite part integrals (in the Hadamard sense). The contours $C^+$, $C^-$, the surface $S_c$ and $y_{max}$ and $y_{min}$ are defined in the text.

$$\iint_{S_c} \frac{1}{r^3}\,dx\,dy = \int_{C^+} \frac{x-R}{y^2R}\,dy + \int_{C^-} \frac{x+R}{y^2R}\,dy - 2\left[\frac{1}{y_{max}} - \frac{1}{y_{min}}\right]$$

$$\iint_{S_c}\frac{x}{r^3}\,dx\,dy=\int_{C^+}\frac{-1}{R}\,dy-\int_{C^-}\frac{1}{R}\,dy$$

$$\iint_{S_c}\frac{y}{r^3}\,dx\,dy=\int_{C^+}\frac{x-R}{yR}\,dy+\int_{C^-}\frac{x+R}{yR}\,dy+2\cdot\ln\left|\frac{y_{max}}{y_{min}}\right|$$

$$\iint_{S_c}\frac{x^2}{r^3}\,dx\,dy=\int_{C^+}\left[\ln(R+x)-\frac{x}{R}\right]dy+\int_{C^-}\left[\ln\left[\frac{R+x}{y^2}\right]-\frac{x}{R}\right]dy$$
$$-2[(y_{max}\cdot\ln|y_{max}|-y_{max})-(y_{min}\cdot\ln|y_{min}|-y_{min})]$$

$$\iint_{S_c}\frac{xy}{r^3}\,dx\,dy=\int_{C^+}\frac{-y}{R}\,dy-\int_{C^-}\frac{y}{R}\,dy$$

$$\iint_{S_c}\frac{y^2}{r^3}\,dx\,dy=\int_{C^+}\frac{x-R}{R}\,dy+\int_{C^-}\frac{x+R}{R}\,dy+2\cdot(y_{max}-y_{min})$$

$$\iint_{S_c}\frac{x^2}{r^5}\,dx\,dy=\int_{C^+}\left[\frac{x-R}{3y^2R}-\frac{x}{3R^3}\right]dy+\int_{C^-}\left[\frac{x+R}{3y^2R}-\frac{x}{3R^3}\right]dy-\frac{2}{3}\cdot\left[\frac{1}{y_{max}}-\frac{1}{y_{min}}\right]$$

$$\iint_{S_c}\frac{xy}{r^5}\,dx\,dy=\int_{C^+}\frac{-y}{3R^3}\,dy-\int_{C^-}\frac{y}{3R^3}\,dy$$

$$\iint_{S_c}\frac{y^2}{r^5}\,dx\,dy=\int_{C^+}\left[2\cdot\frac{x-R}{3y^2R}+\frac{x}{3R^3}\right]dy+\int_{C^-}\left[2\cdot\frac{x+R}{3y^2R}+\frac{x}{3R^3}\right]dy-\frac{4}{3}\cdot\left[\frac{1}{y_{max}}-\frac{1}{y_{min}}\right]$$

$$\iint_{S_c}\frac{x^3}{r^5}\,dx\,dy=\int_{C^+}\left[\frac{-1}{R}+\frac{y^2}{3R^3}\right]dy+\int_{C^-}\left[\frac{-1}{R}+\frac{y^2}{3R^3}\right]dy$$

$$\iint_{S_c}\frac{x^2y}{r^5}\,dx\,dy=\int_{C^+}\left[\frac{x-R}{3yR}-\frac{xy}{3R^3}\right]dy+\int_{C^-}\left[\frac{x+R}{3yR}-\frac{xy}{3R^3}\right]dy+\frac{2}{3}\cdot\ln\left|\frac{y_{max}}{y_{min}}\right|$$

$$\iint_{S_c}\frac{x^4}{r^5}\,dx\,dy=\int_{C^+}\left[\ln(R+x)-\frac{4x}{3R}+\frac{xy^2}{3R^3}\right]dy+\int_{C^-}\left[\ln\left(\frac{R+x}{y^2}\right)-\frac{4x}{3R}+\frac{xy^2}{3R^3}\right]dy$$
$$-2[(y_{max}\cdot\ln|y_{max}|-y_{max})-(y_{min}\cdot\ln|y_{min}|-y_{min})]$$

$$\iint_{S_c}\frac{x^3y}{r^5}\,dx\,dy=\int_{C^+}\left[\frac{-y}{R}+\frac{y^3}{3R^3}\right]dy+\int_{C^-}\left[\frac{-y}{R}+\frac{y^3}{3R^3}\right]dy$$

$$\iint_{S_c}\frac{x^2y^2}{r^5}\,dx\,dy=\int_{C^+}\left[\frac{x-R}{3R}-\frac{xy^2}{3R^3}\right]dy+\int_{C^-}\left[\frac{x+R}{3R}-\frac{xy^2}{3R^3}\right]dy+\frac{2}{3}\cdot(y_{max}-y_{min})$$

$$\iint_{S_c}\frac{xy^2}{r^5}\,dx\,dy=\int_{C^+}\frac{-y^2}{3R^3}\,dy+\int_{C^-}\frac{-y^2}{3R^3}\,dy$$

$$\iint_{S^c}\frac{y^3}{r^5}\,dx\,dy=\int_{C^+}\left[2\cdot\frac{x-R}{3yR}+\frac{xy}{3R^3}\right]dy+\int_{C^-}\left[2\cdot\frac{x+R}{3yR}+\frac{xy}{3R^3}\right]dy+\frac{4}{3}\cdot\ln\left|\frac{y_{max}}{y_{min}}\right|$$

$$\iint_{S_c}\frac{xy^3}{r^5}\,dx\,dy=\int_{C^+}\frac{-y^3}{3R^3}\,dy+\int_{C^-}\frac{-y^3}{3R^3}\,dy$$

$$\iint_{S_c}\frac{y^4}{r^5}\,dx\,dy=\int_{C^+}\left[2\cdot\frac{x-R}{3R}+\frac{xy^2}{3R^3}\right]dy+\int_{C^-}\left[2\cdot\frac{x+R}{3R}+\frac{xy^2}{3R^3}\right]dy+\frac{4}{3}\cdot(y_{max}-y_{min})$$

## REFERENCES


1. I. S. Raju and J. C. Newman Jr., 'Stress-intensity factors for a wide range of semi-elliptical surface cracks in finite-thickness plates', *Eng. Fract. Mech.*, **11**, 817–829 (1979).
2. T. A. Cruse and W. Vanburen, 'Three-dimensional elastic stress analysis of a fracture specimen with an edge crack', *Int. J. Fract. Mech.*, **17**, 1–15 (1971).
3. T. A. Cruse and G. J. Meyers, 'Three-dimensional fracture mechanical analysis', *J. Struct. Div. ASCE*, **103**, 309–320 (1977).
4. J. O. Lachat and J. O. Watson, 'Progress in the use of boundary integral equations illustrated by examples', *Comp. Methods Appl. Mech. Eng.*, **10**, 273–289 (1977).
5. J. Weaver, 'Three-dimensional crack analysis', *Int. J. Solids Struct.*, **13**, 321–330 (1977).
6. H. D. Bui, 'An integral equations method for solving the problem of a plane crack of arbitrary shape', *J. Mech. Phys. Solids*, **25**, 29–39 (1977).
7. C. L. Tan and R. T. Fenner, 'Stress intensity factors for semi-elliptic surface cracks in pressured cylinders using the boundary integral equation method', *Int. J. Fract.*, **16**, 233–245 (1980).
8. M. L. Luchi and S. Rizzuti, 'Boundary elements for three-dimensional elastic crack analysis', *Int. j. numer. methods eng.*, **24**, 2253–2271 (1987).
9. Y. Murakami and S. Nemat-Nasser, 'Interacting dissimilar semi-elliptic surface flaws under tension and bending', *Eng. Fract. Mech.*, **16**, 373–386 (1982).
10. Y. Murakami and S. Nemat-Nasser, 'Growth and stability of interacting surface flaws of arbitrary shape', *Eng. Fract. Mech.*, **17**, 193–210 (1983).
11. J. C. Lee and L. M. Keer, 'Study of a 3-D crack terminating at an interface', *J. Appl. Mech.*, **53**, 311–316 (1986).
12. A. Gerasoulis, 'The use of piecewise quadratic polynomials for the solution of singular integral equations of Cauchy type', *Comp. Math. Appl.*, **8**, 15–22 (1982).
13. S. Krenk, 'On quadrature formulas for singular integral equations of the first and the second kind', *Quart. Appl. Math.*, **33**, 225–232 (1975).
14. P. S. Theocaris, N. I. Iokimidis and J. G. Kazantzakis, 'On the numerical evaluation of 2-D principal value integrals', *Int. J. numer. methods eng.*, **15**, 629–634 (1980).
15. J. Hadamard, *Lectures on Cauchy's Problem in Linear Partial Differential Equations*, Yale University Press, 1923.
16. A. C. Kaya and F. Erdogan, 'On the solution of integral equations with strongly singular kernels', *Quart. Appl. Math.*, **45**, 105–122 (1987).
17. N. I. Ioakimidis, 'Validity of the hypersingular integral equation of crack problems in 3-D elasticity along the crack boundaries', *Eng. Fract. Mech.*, **26**, 783–788 (1987).
18. H. R. Kutt, 'The numerical evaluation of principal value integrals by finite part integration', *Numer. Math.*, **24**, 205–210 (1975).
19. C. A. Brebbia, *The Boundary Element Method for Engineers.*, Pentech Press, London, 1978.
20. S. L. Crouch, 'Solution of plane elasticity problems by the displacement discontinuity method; I. Infinite body solution', *Int. j. numer. methods eng.*, **10**, 301–343 (1976).
21. N. Fares, 'Green functions of plane-layered elastostatic and viscoelastic regions with application to 3-D crack analysis', *Ph. D. Thesis*, Massachusetts Institute of Technology, 1987.
22. N. Fares and V. C. Li, 'General image method in a plane-layered elastostatic medium', *J. Appl. Mech.*, **10**, 781–785 (1988).
23. H. Tada, P. C. Paris and G. R. Irwin, *The Stress Analysis of Cracks Handbook.*, Del. Research Corp., 1973.
24. H. Gao and J. R. Rice, 'Somewhat circular tensile cracks', *Int. J. Fract.*, **33**, 155–174 (1987).